# การวิเคราะห์ความดันรูเล็กข้ามชั้นบางที่แยกฟองในช่องแคบที่ถูกบีบ

# CAPILLARY PRESSURE ANALYSIS ACROSS A LAMELLA SEPARATING BUBBLES IN CONSTRICTED CHANNELS

***นายวิโรจน์ เรืองประเทืองสุข***
*ภาควิชาวิศวกรรมเคมี คณะวิศวกรรมศาสตร์*
*มหาวิทยาลัยบูรพา ชลบุรี 20131*



## บทคัดย่อ

รายละเอียดเชิงปริมาณสำหรับการคำนวณตำแหน่งและความโค้งของชั้นบางระหว่างฟองที่สัมผัสกันในช่องแคบที่ถูกบีบได้ถูกอนุพัทธ์ขึ้นกลุ่มสมการเชิงวิเคราะห์ดังกล่าวจะใช้ในการพิจารณากำหนดค่าการเปลี่ยนแปลงความดันรูเล็กข้ามผิวระหว่างหน้าของแก๊ส-ของเหลว-แก๊ส ที่ไหลในสื่อพรุนของวัฏภาคที่กระจาย (โฟม) แม้ว่าตำแหน่งของผิวระหว่างหน้าแต่ละผิวจะมีผลลัพธ์แม่นตรงในรูปแบบเชิงปริยายที่ซับซ้อนและต้องใช้การคำนวณเชิงตัวเลขที่ยุ่งยาก แต่ยังเป็นไปได้ที่จะประมาณค่าได้อย่างแม่นยำ โดยมีความคลาดเคลื่อนเพียงเล็กน้อยภายใต้ภาวะเชิงปฏิบัติ

## Abstract

The quantitative descriptions for calculating the position and curvature of a lamella between contacted bubbles in constricted channel have been derived. Such analytical epuations provide the determination of capillary pressure change across the gas-liguid-gas interfaces during dispersed phase (foam) flow in porous media. Although the exact results are highly implicit and would require significant numerical calculations at each interface, accurate approximations within a few percent errors are possible under certain practical conditions.

Key words : capillary pressure, foam flow, porous media

## 1. Introduction

When a two-phase system moves through a porous medium, the non-wetting phase tends to be broken down into discontinuous units by various snap-off and phase division processes (Ransohoff, T.C. and Radke, C.J., 1988; Ransohoff, T.C., Gauglitz, P.A. and Radke, C.J., 1987; Mohanty, K.K., 1981; Roof, J.G., 1970). If these fluid phases are devoid of any film stabilizing surface active agents, these bubble (or drop) generation processes are countered by rapid reconnection (coalescence) processes, and the non-wetting phase effectively moves in a pseudo-continuous manner through the porous medium. This continuity of the phases then allows the use of conventional methods for describing multiphase displacement and flow, e.g., the use of fractional flow theory coupled with relative permeability determinations as a function of phase saturations. We refer to such multiphase flows as non-dispersed phase flows.

If a surfactant that significantly inhibits the in situ coalescence processes is present, the non-wetting phase will remain discontinuous and the description of the displacement will depend upon the resident texture (bubble size, bubble size distribution) as well as the phase saturations. This additional dependence on phase texture significantly complicates the analysis of such flows, which we refer to here as dispersed phase flows. No longer is the analysis within the scope of fractional flow theory and new approaches are needed to satisfactorily describe the observed behavior. Currently, this poses a significant new change in multiphase flow phenomena in porous media and in recent years has occupied the interest of a number of investigators (Kovscek, A.R., Patzek, T.W., and Radke, C.J., 1997; Cohen, D., Patzek, T.W., and Radke, C.J., 1996; Willis, M.S., 1995; Goode, P.A. and Ramakrishnan, T.S., 1993; Gennes, P.G., 1992; Gauglitz, P.A. and Radke, C.J., 1990; Rossen, W.R., 1990; Ransohoff, T.C. and Radke, C.J., 1988; Ettinger, R.A. and Radke, C.J., 1989; Prieditis J.C., 1988; Flumerfelt, R.W. and Prieditis, J.C., 1988; Hirasaki, G.J. and Lawson, J.B., 1985; Stover, R.L., Tobias, C.W., and Denn, M.M., 1977; Holm, LW., 1968; Bernard, G.G., Holm, L.W. and Jacobs, W.L., 1965).

We present here the equations for calculating the position and curvature of a lamella between contacted bubbles in constricted channel. We first follow Prieditis (1988) and develop the equations for two dimensional and three dimensional channels with constant sloped walls. The results are then extended to channels with walls which have axially varying slopes. Of particular interest in the latter connection is the channel with a sinusoidally varying radius.

## 2. Two Dimensional Diverging Plate

Consider the two-dimensional geometry of a lamella in a channel formed by two diverging plates as shown in Fig. 1. Zero contact angles are assumed at the gas-liquid-wall contact points $(x_1, y_1)$ and $(x_2, y_2)$ and at the apparent contact point ($C$) between the bubbles and liquid in the plateau border. The quantities $R_1$ and $R_2$ are the radii of curvature at the gas-liquid interfaces between the bubbles and the liquid in the plateau border. The points $(x_1', y_1')$ and $(x_2', y_2')$ are the center points of this radii and are located by the intersections of passing through the points $(x_1', y_1')$, $C$, and $(x_2', y_2')$ which are lines perpendicular to the gas-liquid interfaces.

From the geometry of Fig. 1, it follows that

$$x_1' = x_1 + R_1 \sin\alpha \quad (1)$$

$$y_1' = y_1 \tan\alpha - R_1 \cos\alpha \quad (2)$$

$$x_2' = x_2 + R_2 \sin\alpha \quad (3)$$

$$y_2' = y_2 \tan\alpha - R_2 \cos\alpha \quad (4)$$

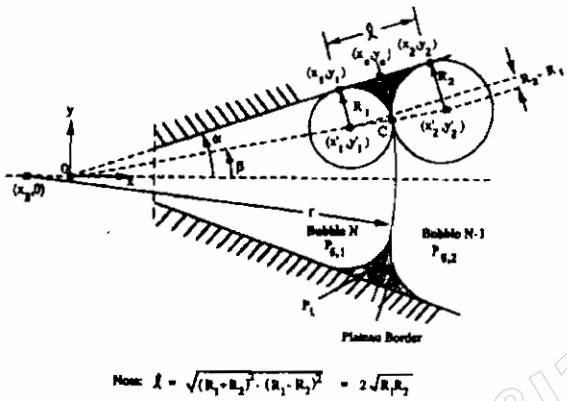


**Fig. 1** Geometry of the two dimensional diverging pore.

From the geometry of Fig. 1, it follows that $x_1$ and $x_2$ are related by

$$x_2 = x_1 + 2\sqrt{R_1 R_2}\cos\alpha \quad (5)$$

and $$m \equiv \tan\beta = y_1'/(x_1' - x_3) \quad (6)$$

Also, the lamella radius "$r$" can be written as

$$r = \frac{y_1'}{\sin\beta} + R_1 = y_1'\left(1 + 1/m^2\right)^{1/2} + R_1 \quad (7)$$

Finally, we applied Laplaces' capillary equation across the gas-liquid interfaces and across the lamella to obtain

$$\Delta P = \frac{2\sigma}{r} = P_{C1} - P_{C2} \quad (8)$$

since $$P_{C1} = \frac{2\sigma}{R_1} \quad , \quad P_{C2} = \frac{2\sigma}{R_2} \quad (9,10)$$

then $$r = \frac{2R_1R_2}{R_2 - R_1} \quad (11)$$

To determine the pressure difference across the lamella, $\Delta P$, we first fix the values of $\alpha$, $x_1$, and $R_1$, and then guess a value for $R_2$. This allows the determinations of $x_1'$, $y_1'$, $x_2'$, $y_2'$, and $x_2$ from Eqs. (1)-(5). We then calculate $x_3$, and $r$ from Eqs. (6)-(7) and update the value of $R_2$ using a Newton-Raphson procedure. Once convergence is obtained, the pressure difference across the lamella is determined from Eq.(8). The result is generally reported in dimensionless form, i.e.,

$$\Delta P_{(2)}^* = 2/r^* \quad (12)$$

where $$\Delta P_{(2)}^* = \frac{\Delta P}{\sigma/R_0} \quad (13)$$

and $$r^* = 2/R_0 \quad (14)$$

while the subscript (2) reminds us that the result is for the two dimensional case. The quantity $R_0$ is a characteristic radius.

### 3. Three Dimensional Axisymmetrical Conical Pore

The geometry for a cone-shaped pore is shown in Fig. 2. The gas-liquid interfaces in the plateau border region are not circular as in the previous two dimensional case. There are instead nodoidal surfaces. Also, the liquid lamella between bubbles is spherical in shape.

For this case, the dimensionless pressure drop across the lamella is

$$\Delta P_{(3)}^* = \frac{\Delta P}{2\sigma/R_0} = P_{C1}^* - P_{C2}^* = 2/r^* \quad (15)$$

where $$P_{C1}^* \equiv P_{C1}/(2\sigma/R_0) \quad (16)$$

and $$P_{C2}^* \equiv P_{C2}/(2\sigma/R_0) \quad (17)$$

From simple geometry and Eq. (15), it follows that

$$R_C^* = r^* \sin\beta = \frac{2\sin\beta}{\Delta P^*} = \frac{2\sin\beta}{P_{C1}^* - P_{C2}^*} \quad (18)$$

In terms of the geometric variables $R^*$ and 0, Laplaces' Equation for the gas-liquid interfaces in the plateau border region can be written as

$$P_C^* = \frac{1}{2}\left(\frac{d}{dR^*}\sin\theta + \frac{\sin\theta}{R^*}\right) = \frac{\sigma}{2R^*}\frac{d}{dR^*}\left(R^*\sin\theta\right) \quad (19)$$

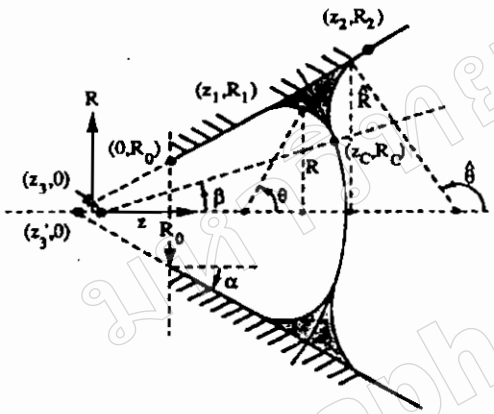


**Fig. 2** Geometry of the three dimensional diverging pore.

Direct integration then gives the equations defining the plateau border interfaces 1 and 2, i.e.,

$$\left(R_1^{*2} - R^{*2}\right)P_{C1}^2 + R^*\sin\theta - R_1^*\cos\alpha = 0 \quad (20)$$

$$\left(R_2^{*2} - \hat{R}^{*2}\right)P_{C2}^2 + \hat{R}^*\sin\hat{\theta} - R_2^*\cos\alpha = 0 \quad (21)$$

where we have used $\hat{R}^*$ and $\hat{\theta}$ to denote $R^*$ and $\theta$ variables on the "2" interface.

Similarly, we can obtain the equation defining the shape of the liquid lamella, where $\sigma$ in Eq. (19) is replaced by $2\sigma$ in this case to account for the 2 interfaces making up the liquid lamella, as

$$R_1^{*2}P_{C1}^* - R_2^{*2}P_{C2}^* - \left(R_1^* - R_2^*\right)\cos\alpha = 0 \quad (22)$$

Applying Eq. (20) at $\theta = \beta$ where $R^* = R_C^*$, and using Eq. (18), gives

$$R_1^* = \frac{\cos\alpha + \sqrt{\cos^2\alpha + 2P_{C1}^*\left[R_C^{*2}\left(P_{C1}^* + P_{C2}^*\right)\right]}}{2P_{C1}^*} \quad (23)$$

Rearranging Eq. (19) gives

$$R_2^* = \frac{\cos\alpha + \sqrt{\cos^2\alpha - 4P_{C2}^*\left(R_1^*\cos\alpha - R_1^{*2}P_{C1}^*\right)}}{2P_{C2}^*} \quad (24)$$

The axial distance $Z_2^* - Z_1^*$ between the intersection points of the interfaces in the conical surface is given by

$$Z_2^* - Z_1^* = \frac{R_2^* - R_1^*}{\tan\alpha} = \int_{R_C^*}^{R_1^*}\tan\theta dR^* + \int_{R_C^*}^{R_2^*}\tan\theta dR^* \quad (25)$$

Using Eqs. (15) and (21),

$$f(\beta) = \int_{\beta}^{\alpha+\pi/2}\frac{R^*\sin\theta}{2R^*P_{C1}^* - \sin\theta}d\theta + \int_{\pi+\beta}^{\alpha+\pi/2}\frac{\hat{R}^*\sin\hat{\theta}}{2\hat{R}^*P_{C2}^* - \sin\hat{\theta}}d\hat{\theta} - \frac{R_2^* - R_1^*}{\tan\alpha} = 0 \quad (26)$$

where $R^*$ in the first integral is obtained from Eq. (20) and $\hat{R}^*$ in the second integral form Eq. (21).

Eq. (26) represents an implicit equation in terms of $\beta$ if $P_{C1}^*$, $P_{C2}^*$ and $\alpha$ are fixed. This equation can be combined with Eqs. (18), (20), (21), (23), and (24) to determine $\beta$ using an iterative Newton-Raphson procedure. Convergence of this procedure to a constant $\beta$ also gives $R_C^*$ from Eq. (18), $R_1^*$ form Eq. (20),

and $R_2^*$ from Eq. (21). The corresponding values of $\Delta P_{(3)}^*$ and $r^*$ are obtained directly from the specified values of $P_{C1}^*$ and $P_{C2}^*$ and Eq. (15).

## 4. Comparison of Two Dimensional and Three Dimensional Cases

In each of the above calculations, three quantities had to be specified before complete shape calculations could be executed. In comparing the two dimensional and three dimensional results, we will compare $\Delta P_{(2)}^*$ and $\Delta P_{(3)}^*$ for specific values of $\alpha$, $P_{C1}^*$, and $Z_1^*$ (or $x_1^*$ in the two dimensional case). In particular, in Fig. 3, we show the results of such calculations. As can be seen that $\Delta P_{(2)}^*$ and $\Delta P_{(3)}^*$ values are nearly identical regardless of the value of $Z_1^*\left(=x_1^*\right)$ and $P_{C1}^*$. The results in Fig. 3 are for a fixed $\alpha$; however, calculations at different $\alpha$'s also showed similar results.

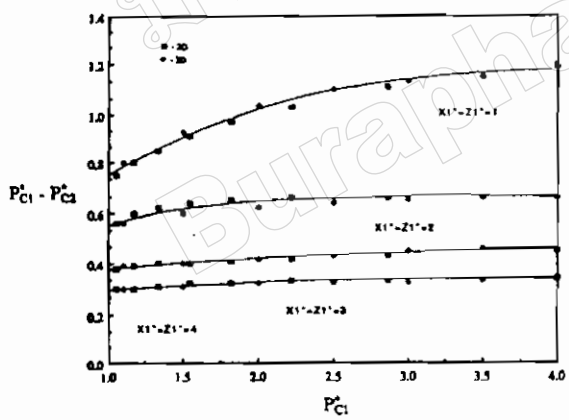


**Fig. 3** Comparison of 2-D and 3-D case studies.

The importance of these results is that we can use simple two dimensional calculations to predict three dimensional results. In particular, if $\Delta P_{(2)}^*$ is determined, then

$$\Delta P_{(3)}^*\left(\alpha, Z_1^*, P_{C1}^*\right) \equiv \Delta P_{(2)}^*\left(\alpha, x_1^*, P_{C1}^*\right) \quad (27)$$

$$\Delta P_{(3)}^* = \frac{2\sigma}{R_0}\Delta P_{(2)}^* \quad (28)$$

In the two dimensional calculations, a further simplifications is possible since it can be shown (theoretically or numerically) that $x_3$ in Fig. 1 is identically zero (Prieditis 1988). Under such conditions,

$$r^* = \frac{x_4^*}{\cos\alpha} \quad (29)$$

here, $x_4^*$ is the axial position of the intersection of the extended lamella curve with the pore wall. From Eq. (12), the pressure difference is then

$$\Delta P_{(2)}^* = 2\cos\alpha / x_1^* \quad (30)$$

Hence, if Eq. (28) is used,

$$\Delta P_{(3)}^* = \frac{Z_4^*}{\cos\alpha} \quad (31)$$

## 5. Two Dimensional Sinusoidal Pore

The geometry of the channel is shown in Fig. 4. The gap R between the two wall varies according to

$$y = a - b\cos\lambda x \quad (32)$$

with $$a = \frac{1}{2}\left(y(0) + y(L)\right) \quad (33)$$

and $$b = \frac{1}{2}\left(y(L) - y(0)\right) \quad (34)$$

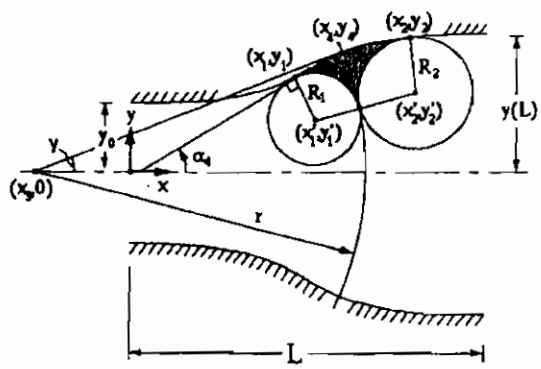


**Fig. 4** Geometry of the two dimensional sinusoidal pore.

where $\lambda = \pi/L$. For the diverging section shown in Fig. 4, $y(0)$ corresponds to $Y_{\min}$ and $y(L)$ corresponds to $Y_{\max}$; for a converging section, this correspondence is reversed.

The slope at any point $(x_i, y_i)$ on the channel surface, $\tan\alpha_i$, can be obtained from

$$\tan\alpha_i = \left.\frac{dy_i}{dx_i}\right|_{x=x_i} = b\lambda \sin\lambda x_i \qquad (35)$$

$$\alpha_i = \tan^{-1}(b\lambda \sin\lambda x_i) \qquad (36)$$

The coordinates for the center points $(x_1', y_1')$ and $(x_2', y_2')$ are:

$$x_1' = x_1 + R_1 \sin\alpha_1 \qquad (37)$$

$$y_1' = a - b\cos\lambda x_1 + R_1 \cos\alpha_1 \qquad (38)$$

$$x_2' = x_1 + R_2 \sin\alpha_2 \qquad (39)$$

$$y_2' = a - b\cos\lambda x_2 + R_2 \cos\alpha_2 \qquad (40)$$

and $$\frac{y_1'}{y_2'} = \frac{r - R_1}{r + R_2} \qquad (41)$$

Substituting Eq. (38) into Eq. (41) gives

$$R_1 = R_2\left(\frac{y_1'}{y_2'}\right) \qquad (42)$$

Also

$$f = (x_2' - x_1')^2 + (y_2' - y_1')^2 = (R_1 + R_2)^2 \qquad (43)$$

If Eqs. (37)-(40) and Eq. (42) are used in Eq. (43), we can eliminate $x_1', x_2', y_1', y_2'$ and $R_1$ and obtain

$$f(x_1, x_2, R_2, \lambda, a, b) = 0 \qquad (44)$$

Further, if we fix $x_1, x_2, L, R(0)$ and $R(L)$, this equation reduces to

$$f(R_2) = 0 \qquad (45)$$

A Newton-Raphson procedure is then used to determine $R_2$, with the other variables following from the previous equations ($x_2'$ from Eq. (39), $y_2'$ from Eq. (40), $R_1$ and $y_1'$ from Eqs. (38) and (42), $x_1'$ from Eq. (37) and $r$ from Eq. (39)).

Once $r$ is determined, the pressure difference across the lamella is given by

$$\Delta P^* = \frac{\Delta P}{\sigma/y(0)} = \frac{2}{r^*} \qquad (46)$$

where

$$r^* = \frac{r}{y(0)} \qquad (47)$$

The point $(x_4, y_4)$ and the slope $\tan\alpha_4$ is then obtained from the simultaneous solution of the equations:

$$\tan\alpha_4 = b\lambda \sin\lambda x_4 \qquad (48)$$

$$\sin\alpha_4 = \frac{y_4}{r} \qquad (49)$$

$$y_4 = a - b\cos\lambda x_4 \qquad (50)$$

Finally, to determine $x_3$, we use

$$\frac{x_4 - x_3}{r} = \sin\alpha_4 \qquad (51)$$

The position $(x_4, y_4)$ is the point where the extended lamella curve intersects the wall. In general, this curve is not perpendicular to the wall at the point of intersection. If $\gamma$ is the angle of a line which is perpendicular to the extended lamella curve at $(x_4, y_4)$, then

$$y_4 = r\sin\gamma \qquad (52)$$

$$x_4 = x_3 + r\cos\gamma \qquad (53)$$

Also, $$y_4 = a - b\cos\lambda x_4 \qquad (54)$$

and $$y_1' = m(x_3 - x_1') \qquad (55)$$

where $$m = \frac{y_2' - y_1'}{x_2' - x_1'} \qquad (56)$$

Solution of these equations gives $x_3, x_4, y_4, \gamma$ and $m$.

## 6. Approximate Solution

In general, $\gamma$ will be different from $\alpha_4$. However, if $\gamma$ is taken to be equal to $\alpha_4$, an approximate solution is obtained. In particular, if we know the position $x_4$, an approximate value $r'$ of the radius $r$ can be obtained from

$$r^{*'} = r^*\Big|_{\gamma=\alpha_i} = \frac{y_4}{\sin\alpha_4} = \frac{a - b\cos\lambda x_4^*}{\sin\alpha_4} \tag{57}$$

The pressure difference is then given by

$$\Delta P^{*'} = \frac{2}{r^{*'}} \tag{58}$$

In Table 1 we compare the values of $\Delta P^*$ and $\Delta P^{*'}$. The $x_4$ value used in each case was the same, i.e., that obtained from the exact solution. We see from the results that only small errors are involved in using Eqs. (57) and (58). This is particularly important if one can estimate the position in $x_4^*$ from a knowledge of the volume of bubble "1" in the channel.

**Table 1.** Comparison of the exact and approximation solutions for the two dimensional sinusoidal pore.

| $x_1^*$ | $x_2^*$ | $\Delta P^*$ | | |
|---|---|---|---|---|
| | | Exact | Approx. | %Error |
| 0.1 | 0.1 | 0.268 | 0.268 | 0.000 |
| 0.5 | 0.7 | 0.877 | 0.879 | 0.228 |
| 1.0 | 1.2 | 0.867 | 0.869 | 0.231 |
| 1.0 | 2.0 | 0.740 | 0.756 | 2.162 |
| 1.5 | 1.7 | 0.687 | 0.687 | 0.146 |
| 2.0 | 2.5 | 0.444 | 0.450 | 1.351 |
| 2.0 | 3.0 | 0.180 | 0.188 | 4.444 |
| 2.5 | 2.7 | 0.240 | 0.244 | 1.667 |
| 2.9 | 3.0 | 0.037 | 0.038 | 2.703 |

Fixed values $Y_{max} = 3.0, Y_{min} = 1.0, L = 3.0$

In previous sections, we showed that the two dimensional and three dimensional results for a constant sloped channel were nearly identical if the $\Delta P_{(2)}$ was scaled to $\sigma/R_0$ and $\Delta P_{(3)}$ was scaled to $2\sigma/R_0$. If $|[R(L)-R(0)]/L|$ is sufficiently small, for a three dimensional axisymmetric sinusoidal channel, similar results would be expected between $\Delta P_{(3)}^*$ and $\Delta P_{(2)}^*$ in the sinusoidal case.

Under this conditions,

$$\Delta P_{(3)}^* \equiv \Delta P_{(2)}^* \equiv \frac{y_4}{\sin\alpha_4} = \frac{a - b\cos(\lambda x_4)}{\sin\alpha_4} \tag{59}$$

Here, if $Z_4 (= x_4)$ can be determined from a knowledge of the value of bubble "1" in the channel, Eq. (59) provides a simple approximate relation for determining $\Delta P_{(3)}^*$

## 7. Conclusion

The principal conclusions of this work are to present the equations and the approximate methodology for calculating the position and curvature of a lamella between contacted bubbles in the channel with a sinusoidally varying radius. Such information is useful in determining the capillary and threshold pressures of foam flow in porous media.

# REFERENCE

Bernard, G.G., Holm, L.W., and Jacobs, W.L., "Effect of Foam on Trapped Gas Saturation and on Permeability of Porous Media to Wedia to Water," *SPEJ* (December), 295-300, 1965.

Cohen, D., Patzek, T.W., and Radke, C.J., "Two-Dimensional Network Simulation of Diffusion-Driven Coarsening of Foam Inside a Porous Medium," *J. Colloid and Interface Sc.* **179,** 357-373, 1996.

Ettinger, R.A. and Radke, C J., "The Influence of Texture on Steady Foam Flow in Berea Sandstone," paper SPE 19688, presented at the 1989 Annual Technical Conference of the SPE, San Antonio, Tx., Oct. 8-11, 1989.

Flumerfelt, R.W. and Prieditis, J.C., "Mobility of Foam in Porous Media," *ACS Symposium Series* **373,** 295-325, 1988.

Gauglitz, P.A. and Radke, C.J., "The Dynamics of Liquid Film Breakup in Constricted Cylindrical Capillaries," *J. Colloid and Interface Sc.* **134,** 14-40, 1990

Gennes, P.G. "Conjectures on Foam Mobilization," *Phys. Chem. Colloids and Int. in Oil Production,* Edited by Toulhoat, H , et al, Paris., 283-287, 1992.

Goode, P.A. and Ramakrishnan, T.S., "Momentum Transfer Across Fluid-Fluid Interfaces in Porous Media : a Network Model," *AIChEJ.* **39** (7), 1124-1134, 1993.

Hirasaki, G.J. and Lawson, J.B., "Mechanisms of Foam Flow in Porous Media : Apparent Viscosity in Smooth Capillaries," *Soc. Pet. Eng. J.*, **25,** 176-90 1985.

Holm, L.W., "The Mechanism of Gas and Liquid Flow Through Porous Media in the Presence of Foam," *SPEJ*(December) 359-69, 1968.

Kovscek, A.R., Patzek, T W., and Radke, C.J., "Mechanistic Foam Flow Simulation in Heterogeneous and Multidimensional Porous Media," *SPEJ.* **2,** 511-526, 1997.

Mohanty, K.K., "Fluids in Porous Media Two-Phase Distributions and Flow," Ph.D. Thesis, University of Minnesota, Minneapolis, 1981.

Prieditis J.C., "A Pore Level Investigation of Foam Flow Behavior in Porous Media," Ph.D. Thesis, University of Houston, Houston, Tx , 1988.

Ransohoff, T.C., and Radke, C.J. "Mechanisms of Foam Generation in Glass-Bead Packs," *SPERE* (May), 573-85, 1988

Ransohoff, T.C., Gauglitz, P.A., and Radke,C.J., "Snap-off of Gas Bubbles in Smoothly Constricted Noncircular Capilaries," *AIChEJ.* 33(No.5), 753-76, 1987.

Roof, J G., "Snap-off of Oil Droplets in Water-Wet Pores," *SPEJ*(March) *Trans. AIME* **249,** 85-90, 1970.

Rossen, W.R., "Theory of Mobilization Pressure Gradient of Flowing Foams in Porous Media I. Incompressible Foam," *J.Colloid and Interface Sc.* **136,** 1-16, 1990.

Rossen, W.R., "Theory of Mobilization Pressure Gradient of Flowing Foams in Porous Media II. Effect of Compressibility," *J. Colloid and Interface Sc.***136,** 17-37,1990.

Rossen, W.R., "Theory of Mobilization Pressure Gradient of Flowing Foams in Porous Media III. Asymmetric Lamella Shapes," *J. Colloid and Interface Sc.* **136,** 38-53,1990.

Stover, R.L., Tobias, C.W., and Denn, M.M., "Bubble Coalescence Dynamics," *AIChEJ.* **43**(10), 2385-2392,1977.

Willis, M.S., "Toward and Improved Theory of Capillary Flow," Ph.D. Dissertation, University of Texas at Austin. 1995.